



Cardiac CT for Measurement of Right Ventricular Volume and Function in Comparison with Cardiac MRI: A Meta-Analysis

Jin Young Kim, MD¹, Young Joo Suh, MD, PhD², Kyunghwa Han, PhD², Young Jin Kim, MD, PhD², Byoung Wook Choi, MD, PhD²

¹Department of Radiology, Dongsan Hospital, Keimyung University College of Medicine, Daegu, Korea; ²Department of Radiology, Research Institute of Radiological Science, Severance Hospital, Yonsei University College of Medicine, Seoul, Korea

Objective: We performed a meta-analysis to evaluate the agreement of cardiac computed tomography (CT) with cardiac magnetic resonance imaging (CMRI) in the assessment of right ventricle (RV) volume and functional parameters.

Materials and Methods: PubMed, EMBASE, and Cochrane library were systematically searched for studies that compared CT with CMRI as the reference standard for measurement of the following RV parameters: end-diastolic volume (EDV), end-systolic volume (ESV), stroke volume (SV), or ejection fraction (EF). Meta-analytic methods were utilized to determine the pooled weighted bias, limits of agreement (LOA), and correlation coefficient (r) between CT and CMRI. Heterogeneity was also assessed. Subgroup analyses were performed based on the probable factors affecting measurement of RV volume: CT contrast protocol, number of CT slices, CT reconstruction interval, CT volumetry, and segmentation methods.

Results: A total of 766 patients from 20 studies were included. Pooled bias and LOA were 3.1 mL (-5.7 to 11.8 mL), 3.6 mL (-4.0 to 11.2 mL), -0.4 mL (5.7 to 5.0 mL), and -1.8% (-5.7 to 2.2%) for EDV, ESV, SV, and EF, respectively. Pooled correlation coefficients were very strong for the RV parameters ($r = 0.87-0.93$). Heterogeneity was observed in the studies ($I^2 > 50\%$, $p < 0.1$). In the subgroup analysis, an RV-dedicated contrast protocol, ≥ 64 CT slices, CT volumetry with the Simpson's method, and inclusion of the papillary muscle and trabeculation had a lower pooled bias and narrower LOA.

Conclusion: Cardiac CT accurately measures RV volume and function, with an acceptable range of bias and LOA and strong correlation with CMRI findings. The RV-dedicated CT contrast protocol, ≥ 64 CT slices, and use of the same CT volumetry method as CMRI can improve agreement with CMRI.

Keywords: Right ventricular function; Volumetry; Computed tomography; Magnetic resonance imaging; Meta-analysis

INTRODUCTION

Functional assessment of the right ventricle (RV) is a determinant of the treatment plan and prognosis in various clinical settings (1-3). In addition to the ejection fraction (EF), volumetric parameters of RV, such as end-diastolic volume (EDV), end-systolic volume (ESV), and stroke volume (SV), are important clinical indicators, for example,

to determine the optimal operating time and predict the postoperative outcome of patients with repaired tetralogy of Fallot and to diagnose arrhythmogenic right ventricular dysplasia (3-5).

The complex geometry of the RV makes reliable measurement of RV volume challenging (6, 7), and echocardiography is often suboptimal for RV assessment. Cardiac magnetic resonance imaging (CMRI) is the

Received July 5, 2019; accepted after revision December 16, 2019.

This work was supported by a faculty research grant of Yonsei University College of Medicine (6-2018-0041).

Corresponding author: Young Joo Suh, MD, PhD, Department of Radiology, Research Institute of Radiological Science, Severance Hospital, Yonsei University College of Medicine, 50-1 Yonsei-ro, Seodaemun-gu, Seoul 03722, Korea.

• Tel: (822) 2228-7400 • Fax: (822) 2227-8337 • E-mail: rongzusuh@gmail.com

This is an Open Access article distributed under the terms of the Creative Commons Attribution Non-Commercial License (<https://creativecommons.org/licenses/by-nc/4.0>) which permits unrestricted non-commercial use, distribution, and reproduction in any medium, provided the original work is properly cited.

gold standard to evaluate RV volume and function with high reproducibility (8). However, CMRI has limitations in patients with poor compliance for long scan times or contraindications to CMRI (9). With the recent improvements in the temporal and spatial resolution of computed tomography (CT) scanners, cardiac CT can be used to assess RV volume and function (10). Previous studies that compared CT measurements of RV volume and function with CMRI as the reference standard showed variable results regarding the agreement between cardiac CT and CMRI (6, 11-29). These variable results may be attributable to the differences in RV segmentation methods in cardiac CT and MRI; for example, two-dimensional (2D)- vs. three-dimensional (3D)-based methods, manual vs. semiautomatic vs. automatic segmentation, and threshold-based segmentation vs. simplified contouring (30-33). Considering the clinical significance of RV volume and function, factors affecting the difference and agreement of the measured values on CT and CMRI should be identified through a meta-analysis.

Therefore, the purpose of this meta-analysis was to evaluate the agreement of cardiac CT with CMRI in the assessment of RV volume and functional parameters.

MATERIALS AND METHODS

Our methods followed the Preferred Reporting Items for Systematic Reviews and Meta-Analyses recommendations (34).

Literature Search

A systematic search of the PubMed, EMBASE, and Cochrane library databases was performed to identify relevant studies published till January 9, 2019. Supplementary Materials lists the searched terms.

Study Selection

The articles were independently reviewed by two authors experienced in meta-analyses (4 and 7 years of experience in cardiothoracic radiology). Figure 1 summarizes the literature search process. The inclusion criterion used at

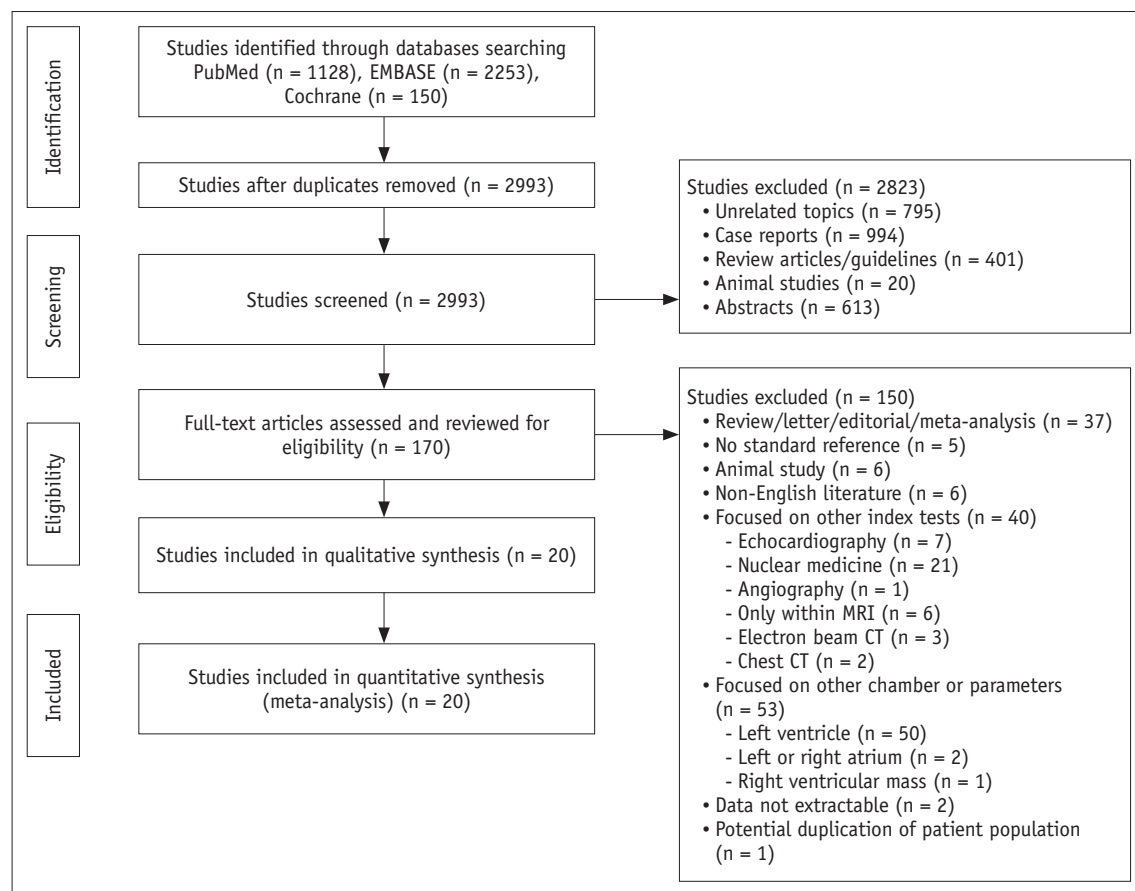


Fig. 1. Flowchart of literature review process. Process of identification and selection of studies for inclusion in this meta-analysis based on Preferred Reporting Items for Systematic Reviews and Meta-Analyses recommendations. CT = computed tomography, MRI = magnetic resonance imaging

the full-text level was a comparison of CT with CMRI as the standard reference in at least one of the following parameters of RV function: EF, EDV, ESV, or SV. The exclusion criteria were the absence of CMRI and other reference standards for RV measurement, use of an index test other than CT, assessment of a cardiac chamber other than RV, incomplete dataset, animal studies, non-English language, potential duplication of patient population, and manuscript format other than original article.

Data Extraction

Data were independently extracted by two investigators. The extracted parameters were: 1) article information and demographic characteristics; 2) acquisition protocol for CT and CMRI: number of CT slices, electrocardiogram (ECG)-gating method during CT, contrast administration protocol in CT (RV-dedicated [triphasic or split-bolus technique] or non-RV-dedicated), reconstruction interval of RR on CT, CMRI scanner type (3 tesla [T] or 1.5T), acquisition sequence for cine image on CMRI; 3) analysis method for RV function: details of the segmentation methods (2D with Simpson's method vs. 3D, manual vs. semiautomatic vs. automatic, threshold-based vs. simplified contouring, inclusion vs. exclusion of trabeculation or papillary muscle in the RV cavity), reconstructed slice thickness, and analysis software tool; 4) study outcomes: results of the Bland-Altman test (bias with 1 or 1.96 standard deviation [SD]) and correlation coefficient between CT and CMRI for EDV, ESV, SV, and EF.

Quality Assessment

The modified Quality Assessment of Diagnostic Accuracy Studies-2 (QUADAS-2) tool was used to assess the study quality (35). Two independent investigators reviewed studies for quality assessment and reached consensus through discussion.

Statistical Analysis

RV parameters measured with CT were compared with CMRI as the standard reference. For each study, bias (mean difference) was calculated by subtraction of the mean of each parameter measured by CT and CMRI, and limits of agreement (LOA) was defined as the SD of the mean difference multiplied by 1.96. The pooled bias and 95% LOA from the included studies were estimated based on the method proposed by DerSimonian and Laird (36). Pooled estimates of the bias and the SD for the difference were

obtained on the basis of the random-effects model, after which 95% LOA was obtained by the method in Williamson et al. (37). The pooled correlation coefficient was analyzed using the inverse variance-weighted method in the DerSimonian-Laird random-effects model. If the results were presented in subgroups in the study, the average bias of the group was used, and the correlation coefficient of each subgroup was integrated by Fisher's *-z*-transformation method (37). Meta-analysis results of bias and LOA for each parameter were drawn as a modified forest plot, in which each circle indicated a study, with the circle size representing the weight (sample size and variance) of each study. Results of pooled correlation coefficients of each parameter were drawn as a forest plot. Heterogeneity was assessed using chi-squared-based *Q* statistics and *I*² statistics (36, 38). For subgroup analysis of factors affecting the agreement in RV measurement, differences in the degree of heterogeneity for correlation coefficients between subgroups were assessed using the Cochran's *Q* test, and the influencing factors were analyzed using a meta-regression analysis. Publication biases were assessed using the Egger's test and drawn as funnel plots (39, 40). The analysis was performed using R (Version 3.5.2, R Foundation for Statistical Computing, Vienna, Austria) with the meta package (41).

RESULTS

Study Characteristics

After the study selection process, a total of 766 patients from 20 studies were included in the meta-analysis (6, 11-29). EDV and ESV were analyzed in all 20 studies, and SV and EF were analyzed in 15 and 19 studies, respectively. Table 1 and Supplementary Table 1 summarize the study characteristics and details of image acquisition and RV analysis method in the included studies. The radiation dose from cardiac CT was 2.7-20 mSv in the ten included studies (11, 15, 16, 20-22, 24-27).

Koch et al. (11) compared two different CT volumetric analysis methods (Simpson's method and the 3D threshold-based segmentation method) in the patient population. In this meta-analysis, results from 3D threshold-based segmentation methods were included to avoid data duplication. Data from the 2D-based Simpson's method were included only in the subgroup analysis for the volumetry method. Guo et al. (18) divided patients in two subgroups based on the presence of mitral regurgitation,

Table 1. Study Characteristics

First Author (Reference Number)	Journal	Year	Study Design	Patient Description [§]	Total No. of Patients Reported	No. of Excluded Patient and Reason [§]	Included No. of Patients in Analysis	Sex (M:F)	Age (Years)	Time between CT and MRI (Days)	CT Scanner	MRI Scanner
Koch (11)	<i>Eur Radiol</i>	2005	Prospective	Suspected CAD (1), follow up after coronary artery bypass graft (18)	19	Due to artifact (1)	18	14:5*	Mean 69 (46–79) [†]	0 [†]	16-slice CT (MX 8000 IDT, Philips)	1.5T (Magnetom Sonata, Siemens)
Lembcke (12)	<i>Ann Thorac Surg</i>	2005	Retrospective	For preoperative diagnosis (25, 12 had RV dysfunction)	25	-	25	18:7	54.9 ± 13.7	1.2 ± 0.8 (0–2) [†]	8- or 16-slice CT (Aquilion Fx Pro, Toshiba)	1.5T (Magnetom Vision, Siemens)
Raman (14)	<i>Am J Cardiol</i>	2005	Prospective	Congenital heart disease (14)	14	-	14	7:7	31.4 ± 10.3	< 90	16-slice CT (LightSpeed-16, GE)	1.5T (CVi, GE)
Raman (13)	<i>Am Heart J</i>	2006	Prospective	Suspected CAD (24)	24	RV inadequate opacification (6)	18	15:9*	60 ± 12*	0	16-slice CT (LightSpeed-16, GE)	1.5T (CVi, GE)
Plumhans (15)	<i>AJR Am J Roentgenol</i>	2008	Prospective	Suspected CAD (38)	38	-	38	25:13	55.0 ± 8.8	0	64-slice CT (SOMATOM Sensation 64 cardiac, Siemens)	1.5T (Gyroscon Intera, Philips)
Schroeder (16)	<i>Clin Res Cardiol</i>	2009	Prospective	Left ventricular EDV > 150 mL (24)	24	-	24	14:10	64.8 ± 9.5	< 2	16-slice CT (Sensation, Siemens)	1.5T (Gyroscon ACS-NT, Philips)
Müller (17)	<i>Eur Radiol</i>	2009	Prospective	Suspected CAD (50)	50	-	50	34:16	62 ± 9 (41–78) [†]	0 (n = 32) or 1 (n = 18)	16-slice CT (Aquilion, Toshiba)	1.5T (Magnetom Sonata, Siemens)
Guo (19)	<i>Int J Cardiol</i>	2010	Retrospective	Suspected CAD (47)	47	-	47	28:19	49 ± 11 (median 50, 35–74) [†]	0	64-slice CT (Brilliance 64, Philips)	1.5T (Magnetom Sonata, Siemens)
Sugeng (6)	<i>JACC Cardiovasc Imaging</i>	2010	NR	Congestive heart failure (9), secondary pulmonary hypertension (7), primary arterial hypertension (5), congenital heart disease (4), CAD (3)	28	-	28	19:9	53 ± 18	0	16-slice CT (Toshiba)	1.5T (Siemens)
Jensen (20)	<i>Eur Radiol</i>	2011	Retrospective	Suspected CAD (33)	33	-	33	27:6	61.0 ± 7.2	0	DSC (SOMATOM Definition, Siemens)	1.5T (Magnetom Avanto, Siemens)
Huang (21)	<i>Int J Cardiovasc Imaging</i>	2012	Retrospective	Suspected pulmonary artery disease (50)	50	-	50	23:27	55.0 ± 9.6	0	320-slice CT (Aquilion ONE, Toshiba)	1.5T (Magnetom Sonata, Siemens)

Table 1. Study Characteristics (Continued)

First Author (Reference Number)	Journal	Year	Study Design	Patient Description [§]	Total No. of Patients Reported	No. of Excluded Patient and Reason [§]	Included No. of Patients in Analysis	Sex (M:F)	Age (Years)	Time between CT and MRI (Days)	CT Scanner	MRI Scanner
Takx (22)	<i>Eur J Radiol</i>	2012	Prospective	Suspected CAD (20)	20	-	20	16:4	60.6 ± 6.5 (50-69) [†]	0	2nd generation DSCT (SOMATOM Definition Flash, Siemens)	1.5T (Magnetom, Avanto, Siemens)
Fuchs (25)	<i>J Cardiovasc Comput Tomogr</i>	2012	Prospective	Post-myocardial infarction (53)	53	Missing part of ventricles (1), improper segmentation by software (1)	51	40:13*	61 ± 10 (34-81) ^{*†}	0-19*	64-slice CT (Aquilion, Toshiba)	1.5T (Avanto, siemens)
Gao (24)	<i>Eur J Radiol</i>	2012	Prospective	COPD and cor pulmonale (63)	63	Unable to perform repeated breath holding during MRI (5)	58	39:19	64 ± 9 (35-78) [†]	0	64-slice CT (LightSpeed VCT, GE)	1.5T (Sonata, Siemens)
Lee (23)	<i>Acad Radiol</i>	2012	Prospective	For assessment of cardiac function (30)	30	-	30	14:16	61.9 ± 11.2	< 7	64-slice CT (Sensation 64, Siemens)	1.5T (Magnetom Avanto, Siemens)
Maffei (28)	<i>Eur Radiol</i>	2012	Prospective	Suspected CAD (79)	79	-	79	46:33	58 ± 17 (median 58, 24-89) [†]	< 7	64-slice CT (Sensation 64, Siemens)	1.5T (Achieva, Philips)
Zhang (26)	<i>Chin Med J (Engl)</i>	2012	Prospective	Rheumatic mitral stenosis (43)	43	-	43	20:23	51 ± 8 (37-74)	0	64-slice CT (Brilliance 64, Philips)	1.5T (Magnetom Sonata, Siemens)
Guo (18)	<i>Int J Cardiol</i>	2013	Prospective	Suspected CAD without MR (30), with MR (54)	84	-	84	40:44	Patients without MR: 41 ± 13 (30-73) [†] , patients with MR (M: 39 ± 11 [28-64] [†] , F: 41 ± 13 [19-65] [†])	0	64-slice CT (Brilliance 64, Philips)	1.5T (Sonata, Siemens)
Wang (29)	<i>J Nucl Cardiol</i>	2013	Prospective	Patients with pulmonary hypertension	23	-	23	4:19	31.7 ± 11.5	< 7	64-slice CT (biograph, Siemens)	1.5T (Magnetom Avanto, Siemens)
Yamasaki (27)	<i>Eur Radiol</i>	2014	NR	Repaired tetralogy of Fallot (33)	33	-	33	19:14	28.9 ± 13.1	0	256-slice CT (Brilliance iCT, Philips)	3T (Achieva 3.0T, Philips)

*Only data of entire population was reported, [†]Means 25th percentile to 75th percentile, [‡]CT and MRI were performed on same day, except in one patient, [§]Data in parentheses indicate number of patients. CAD = coronary artery disease, COPD = chronic obstructive pulmonary disease, CT = computed tomography, DSCT = dual-source CT, EDV = end-diastolic volume, F = female, M = male, MR = mitral regurgitation, MRI = magnetic resonance imaging, NR = not reported, RV = right ventricle, T = tesla

and the results for the entire population, estimated from each subgroup, were used for this meta-analysis. Most of the studies included in this meta-analysis used 2D-based Simpson's methods with the simplified contouring method in CMRI for RV analysis; however, the segmentation methods used in CT differed from study to study.

Table 2. Weighted Bias with LOA and Correlation Coefficients of Right Ventricular Function between Cardiac CT and CMRI

RV Parameters	Weighted Bias	95% LOA*	Correlation Coefficient (95% CI)
EDV (mL)	3.036	17.501 (-5.715–11.786)	0.93 (0.89–0.96)
ESV (mL)	3.589	15.172 (-3.997–11.175)	0.93 (0.89–0.95)
SV (mL)	-0.385	10.675 (-5.722–4.953)	0.88 (0.79–0.93)
EF (%)	-1.763	7.932 (-5.729–2.203)	0.87 (0.79–0.92)

*Data are presented as width of 95% LOA (upper LOA, lower LOA). CI = confidence interval, CMRI = cardiac MRI, EF = ejection fraction, ESV = end-systolic volume, LOA = limits of agreement, SV = stroke volume

Agreement between CT and MRI for Measurements of RV Volume and Function

Table 2 summarizes the weighted bias and LOA for each parameter, and Figure 2 summarizes the modified forest plots as Bland–Altman plots. For EDV, ESV, SV, and EF, the pooled bias was 3.036 mL, 3.589 mL, -0.385 mL, and -1.763%, respectively, and the pooled LOA were -5.715 to 11.786 mL, -3.997 to 11.175 mL, -5.722 to 4.953 mL, and -5.729 to 2.203%, respectively. Significant heterogeneity was observed in all studies ($I^2 > 50\%$, $p < 0.1$).

Correlation between CT and MRI for Measurements of RV Volume and Function

Table 2 summarizes the pooled correlation coefficient of each RV volumetric parameter, and Supplementary Figure 1 summarizes the forest plots. The pooled correlation coefficients of EDV, ESV, SV, and EF were 0.93 (95% confidence interval [CI]: 0.89–0.96), 0.93 (95% CI: 0.89–0.95), 0.88 (95% CI: 0.79–0.93), and 0.87 (95% CI:

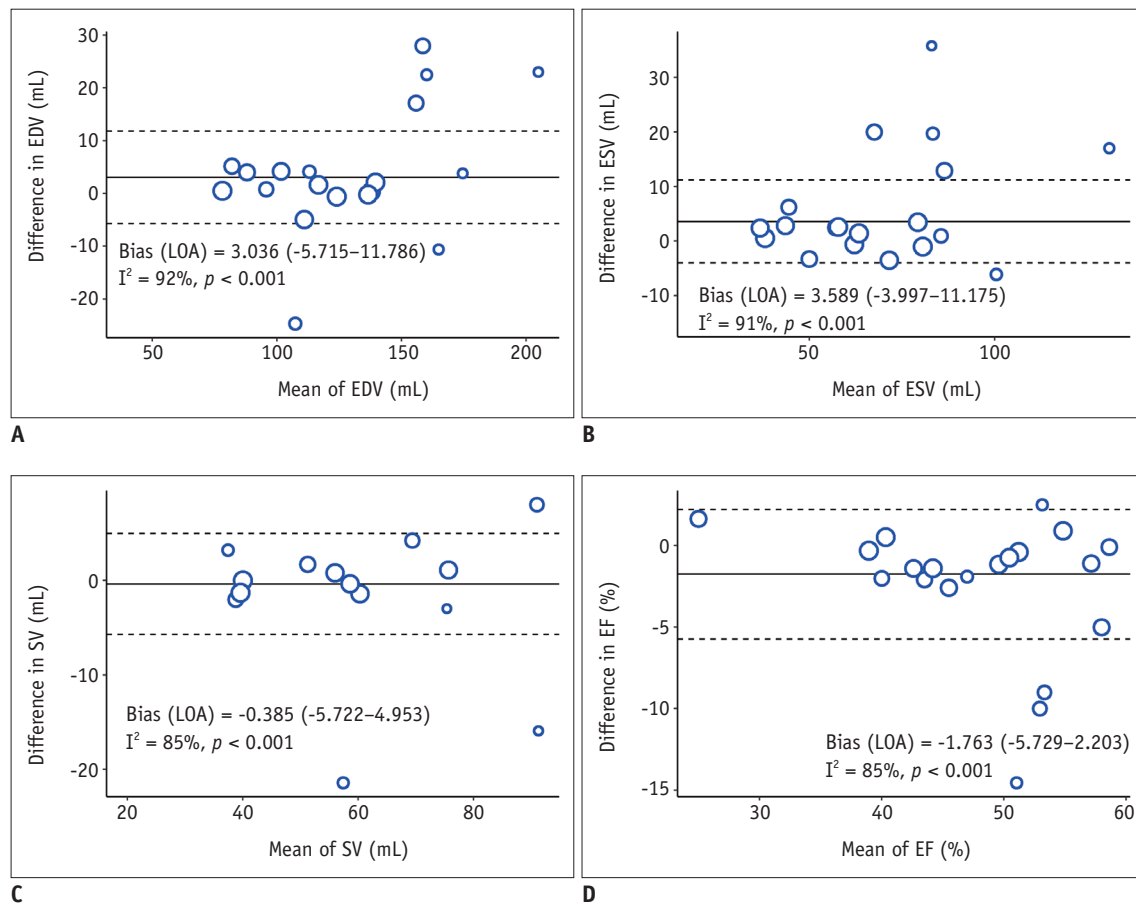


Fig. 2. Modified Bland–Altman plot for agreement between CT and CMRI for RV parameters.

A. EDV. B. ESV. C. SV. D. EF. CMRI = cardiac MRI, EDV = end-diastolic volume, EF = ejection fraction, ESV = end-systolic volume, LOA = limits of agreement, RV = right ventricle, SV = stroke volume

0.79–0.92), respectively. Heterogeneity was observed in all studies ($I^2 > 50\%$, $p < 0.1$).

Subgroup Analysis

Table 3 presents the weighted bias and LOA of subgroup analyses, and Supplementary Figure 2 presents the forest plots for correlation coefficients in subgroup analyses. For correlation coefficients, there were no significant differences in heterogeneity between the subgroups for any parameter, and no significant factors affecting heterogeneity were revealed in the meta-regression ($p > 0.05$) (Supplementary Table 2).

Among the 20 studies, 7 studies (11, 20, 22-24, 27, 29) used an RV-dedicated CT contrast administration protocol and 11 studies (6, 12-14, 17-19, 21, 25, 26, 28) used the non-RV-dedicated contrast protocol. Two studies did not accurately describe the contrast protocol (15, 16). Studies with RV-dedicated CT contrast protocols showed a lower weighted bias and narrower LOA in EDV and SV compared to those with non-RV-dedicated contrast protocols. The weighted bias and LOA of ESV and EF were smaller between the subgroups. The highest correlation coefficient was observed for EDV and ESV with an RV-dedicated contrast protocol ($r = 0.95$ for both). Other RV volume and function parameters showed very strong correlations ($r > 0.8$), regardless of the contrast protocol.

The number of CT slices was ≥ 64 (15, 18-29) in 13 studies and < 64 in 7 studies. In studies with ≥ 64 CT slices (6, 11-14, 16, 17), EDV and ESV showed a lower weighted bias and narrower LOA than in studies with < 64 CT slices. SV and EF showed similar values of weighted bias and LOA between the subgroups. All parameters showed very strong correlations ($r > 0.8$); however, studies with ≥ 64 CT slices showed higher correlation coefficients than those with < 64 CT slices. The CT reconstruction interval was 10% and 5% of the RR intervals in 10 studies (6, 11, 13, 17-19, 21-23, 27) and 9 studies (12, 14-16, 20, 21, 25, 28, 29), respectively. One study did not demonstrate the exact reconstruction interval (24). There were no parameters showing difference in agreement between the subgroups. The RV parameters showed very strong correlations in both subgroups ($r > 0.8$).

The Simpson's method was used in 14 studies for RV volume measurement on CT (12-20, 22, 24, 26, 28, 29), while 3D-based methods were used in 5 studies (6, 21, 23, 25, 27), and Koch et al. (11) used both methods in the same study population. Studies using Simpson's method showed a lower bias and narrower LOA for EDV and ESV than

Table 3. Weighted Bias with LOA of RV Function between Cardiac CT and MRI in Subgroup Analysis

Subgroup	Contrast Protocol		CT Scanner Type		CT Reconstruction Interval		CT Volumetry Method		Segmentation Method	
	Non-RV Dedicated Contrast Protocol	RV Dedicated Contrast Protocol	CT Slice Number < 64	CT Slice Number ≥ 64	5% of RR Interval	10% of RR Interval	Simpson's Method	3D-Based Method	Exclusion of Papillary Muscle and Trabeculation	Inclusion of Papillary Muscle and Trabeculation
EDV (mL)	3.887 (-7.749–15.524)	1.148 (-10.149–12.445)	6.152 (-8.605–20.908)	2.293 (-5.609–10.195)	3.901 (-5.538–13.340)	2.575 (-8.567–13.718)	1.384 (-2.994–5.762)	7.520 (-30.487–45.527)	0.447 (-27.301–28.194)	1.499 (-4.052–7.050)
ESV (mL)	2.978 (-5.601–11.557)	4.994 (-5.048–15.035)	5.339 (-6.396–17.074)	3.312 (-3.693–10.316)	4.079 (-5.424–13.581)	3.706 (-4.411–11.823)	2.175 (-3.026–7.376)	8.196 (-14.713–31.104)	5.035 (-8.353–18.424)	2.570 (-3.327–8.468)
SV (mL)	-6.962 (-24.405–10.481)	0.725 (-3.493–4.943)	-0.253 (-5.245–4.739)	-0.404 (-5.701–4.893)	-2.231 (-11.001–6.540)	0.392 (-3.578–4.363)	-0.110 (-3.190–2.969)	-2.244 (-17.357–12.870)	-5.952 (-23.343–11.440)	-0.095 (-3.252–3.062)
EF (%)	-2.762 (-8.864–3.341)	-0.902 (-3.661–1.857)	-2.208 (-8.011–3.594)	-1.624 (-5.226–1.978)	-1.933 (-7.007–3.141)	-1.777 (-5.601–2.047)	-1.318 (-4.964–2.329)	-2.836 (-8.992–3.320)	-4.280 (-14.143–5.582)	-0.915 (-3.763–1.933)

Data are presented with weighted bias with LOA. 3D = three-dimensional

those using a 3D-based method. SV and EF showed smaller differences in the pooled bias between the subgroups. The parameters showed very strong correlations in both subgroups ($r > 0.8$).

Five studies excluded the papillary muscle and trabeculation from the RV cavity (11, 12, 16, 17, 23), while 12 studies included them in contouring of the RV endocardial border (6, 15, 18-22, 24, 26-28). Three studies did not mention the segmentation method (13, 14, 25). With including the papillary muscle and trabeculation, ESV, SV, and EF showed a lower bias and narrow LOA. EDV showed similar values of bias and LOA between the subgroups. The parameters showed strong correlations ($r \geq 0.8$), except SV and EF using the exclusion method ($r = 0.79$ and 0.76).

Quality of Studies

Figure 3 summarizes the findings for the domains of the QUADAS-2 checklist. Most studies (95%) enrolled consecutive patients. One study did not explain the patient enrollment method (12). The risk of bias was judged as “unclear” in “index test” or “reference standard” domains in eight studies (40%), because there was no mention of whether the CT and CMRI results were interpreted with knowledge of each other (11, 16, 18, 22, 24, 26, 27, 29). Four studies (20%) showed a high risk of bias in the “flow” and “timing” domains, as some patients were excluded from the analysis (11, 13, 24, 25). Concerns regarding applicability were rated “low” in all the domains.

Publication Bias

Supplementary Figure 3 presents the funnel plots of each parameter. EDV and SV showed relatively symmetric

funnel plots without significant publication bias ($p > 0.05$); however, ESV and EF showed significant publication bias ($p = 0.02$ and $p = 0.01$, respectively).

DISCUSSION

Our meta-analysis demonstrates that evaluation of RV functional parameters on CT shows good agreement and very strong correlations with CMRI, although significant heterogeneities are observed in the studies. The RV parameters show a weighted bias < 4 , with overestimation of EDV and ESV and underestimation of EF on CT, and a correlation coefficient > 0.8 . Regarding factors affecting the measurements of RV volume and function, the RV-dedicated CT contrast protocol, CT scanner type with number of slices ≥ 64 , use of CT segmentation with the Simpson’s method, and inclusion of the papillary muscle and trabeculation for contouring the RV endocardial border contribute to better agreement between CT and CMRI.

A previous meta-analysis reported a good agreement and strong correlation between cardiac CT and CMRI for measurement of EF (pooled bias, 4.67%; LOA, 3.71–5.62%; correlation coefficient, 0.79) (42). However, the accuracy of other RV functional parameters, such as EDV, ESV, and SV, was not analyzed using the meta-analytic method before.

Echocardiography is the first-line method for functional evaluation of RV; however, it has limitations because of the position and complex geometry of RV (43, 44). Furthermore, 2D-based fractional area changes on echocardiography cannot fully represent RV global function, and Doppler-derived parameters have an angle dependency (44). Although recent studies reported that 3D echocardiography can accurately

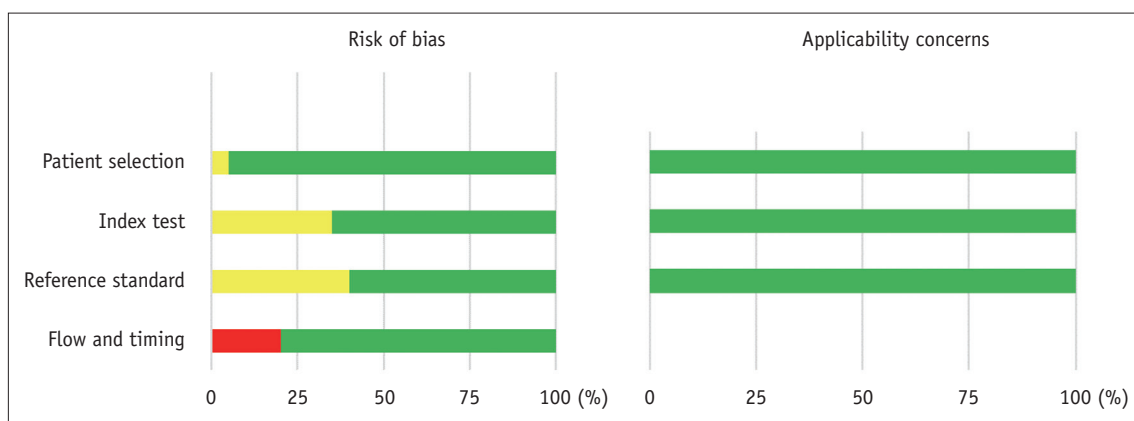


Fig. 3. Quality assessment of included studies. Risk of bias and applicability of concerns domains are presented as percentages based on modified Quality Assessment of Diagnostic Accuracy Studies-2 tool. Each bar shows percentage of studies with high (red), unclear (yellow), and low (green) risks of bias and applicability of concerns.

measure RV volume, it depends on the image quality, and it underestimates RV volume in comparison with CMRI (45).

CMRI is considered as the reference standard; however, the technique is contraindicated in some patients, such as those with implantable or supporting devices and claustrophobia (46). With the development of ECG-gated cardiac CT, 3D volumetric images of the heart can be obtained with high spatial resolution within a short scan acquisition time; therefore, CT can be an alternative tool for cardiac chamber function evaluation in patients who cannot undergo CMRI (47, 48). Although the use of iodinated contrast media and radiation exposure can be disadvantages of CT, recent developments in dose reduction techniques (e.g., image acquisition at low tube voltages with automated exposure control of tube current combined with iterative reconstruction) and low-dose contrast agent administration combined with low tube voltage acquisition can reduce these concerns (49-51).

Therefore, many individual studies investigated the agreement between CT and CMRI for volume and functional measurement of cardiac chambers, including RV (6, 11-29). However, the results for agreement and difference between the two modalities varied across studies. Therefore, we conducted a subgroup analysis based on the factors affecting RV volume and function measurements on CT. Protocols for image reconstruction and segmentation of the RV were almost uniform for CMRI among the included studies. In contrast, CT protocols vary based on the purpose of the exam or depend on the individual institution (52).

Accurate delineation of the RV endocardial contour requires homogeneous enhancement of the RV cavity (48). Since routine coronary CT protocol targets optimal enhancement of the coronary arteries and aorta, a contrast administration protocol focusing on visualizing the right cardiac chamber, such as multiphasic contrast injection or split-bolus technique, can help accurately draw the RV endocardial contour (53). In our study, EDV and SV showed better agreement in the subgroup of RV-dedicated contrast protocol. A contrast protocol focused on RV can be important for accurate evaluation of volume and function. Moreover, the inferior temporal resolution of CT to CMRI may lead to inaccurate ventricular volumetry values, which may be more prominent in previous CT scanners with < 64 slices. In this meta-analysis, studies with ≥ 64 CT slices showed better agreement of EDV and ESV than studies with < 64 CT slices.

The correct determination of end-diastolic and end-

systolic phases is important for accurate measurement of ventricular volume (32, 54). The optimal reconstruction interval of cardiac CT has not been established, but it usually differs by 5% or 10% of the RR interval. Although the 5% interval reconstruction method may be expected to help accurate selection of the end-diastolic/end-systolic phase of the cardiac cycle better than the 10% interval, this meta-analysis showed that the reconstruction interval did not affect the evaluation of RV function on CT.

The volumetry method can be divided into the 2D-based Simpson's method and 3D-based method. In CMRI measurement, the 2D-based Simpson's method is commonly used. However, it shows disadvantages such as incorrect basal slice selection and respiratory misregistration artifacts. Nevertheless, agreement was better in the RV functional parameters when the same method as CMRI (Simpson's method) was used in CT volumetry. Moreover, there was a tendency for overestimation of EDV and ESV in the 3D-based method on CT compared to 2D-based CMRI. This result mainly depends on the difference in principles between the two volumetry methods, since the 2D-based Simpson's method calculates the chamber volume by multiplying the cross-sectional area of each short-axis slice by slice thickness plus inter-slice gap and fails to truly reflect the full anatomical detail of RV. In this context, we should note that 2D CMRI may not represent the actual volume of the cardiac chamber because it mainly relies on the Simpson's method, as shown in a phantom study (6), even CMRI is currently accepted as the reference standard. In addition to the volumetry method, the early timing of the end-diastolic phase with CMRI compared with cardiac CT and the partial volume effects of CT segmentation could be factors resulting in the overestimation of volume with CT, particularly with right ventricular EDV (54).

Moreover, CT attenuation of RV can be a contributing factor, since 3D-based volumetry methods are mostly performed using a threshold-based, region-growing method, which relies on CT attenuation of the RV cavity after contrast administration. However, segmentation with CT images can lead to blurring of the endocardial contour and contain larger parts of the myocardium in the RV cavity in comparison with CMRI, especially in cases of the CT contrast protocol focused on examining the coronary artery (25). Koch et al. (11) compared the two methods in the same patient population and showed insufficient correlation in the 3D-based method, with inhomogeneous contrast enhancement of RV as the probable reason.

Previous studies on ventricular volumetry with CMRI reported that inclusion of the papillary muscle and trabeculation resulted in significant differences in left ventricular volume measurement, up to 25% for EDV and 68% for ESV, and in RV volume measurement, up to 15% for the EDV index and 21% for ESV (30, 33, 55, 56). Although the inclusion of the papillary muscle may overestimate the RV volume, most studies in this meta-analysis included the papillary muscle and trabeculation in the RV cavity with CMRI, while the methods used with CT differed among studies. This meta-analysis showed better agreement in all RV functional parameters when the papillary muscle and trabeculation were included in the RV cavity on CT, probably because of the same segmentation method used in CT and CMRI.

There are several limitations in this meta-analysis. First, the patient characteristics including disease category were different among studies. Second, other variables that could affect the accuracy of RV volume, such as slice thicknesses of CT and CMRI and magnetic field strength of CMRI, were not considered, as most included studies applied the same slices for image reconstruction in CT and CMRI, and used the 1.5T MRI scanner. Third, significant heterogeneity was observed in all studies in this meta-analysis. Although we performed a subgroup analysis for the associated factors, heterogeneity in all subgroups was significant. Finally, the segmentation methods used with CMRI were uniform in this study, and studies with 3D-CMRI were not included because no study met the eligibility criteria.

In conclusion, cardiac CT is reliable for measurement of RV volume and function compared to CMRI, although significant inter-study heterogeneity is observed. Moreover, an RV-dedicated CT contrast protocol, ≥ 64 CT slices, and use of the same CT volumetric method as CMRI (Simpson's method and inclusion of the papillary muscle and trabeculation in the RV cavity) can improve agreement with CMRI.

Supplementary Materials

The Data Supplement is available with this article at <https://doi.org/10.3348/kjr.2019.0499>.

Conflicts of Interest

The authors have no potential conflicts of interest to disclose.

Acknowledgments

We thank Na Won Kim, PhD (Yonsei University Medical Library) for her assistance in literature search.

ORCID iDs

Young Joo Suh

<https://orcid.org/0000-0002-2078-5832>

Jin Young Kim

<https://orcid.org/0000-0001-6714-8358>

KyungHwa Han

<https://orcid.org/0000-0002-5687-7237>

Young Jin Kim

<https://orcid.org/0000-0002-6235-6550>

Byoung Wook Choi

<https://orcid.org/0000-0002-8873-5444>

REFERENCES

- de Groote P, Millaire A, Foucher-Hossein C, Nugue O, Marchandise X, Ducloux G, et al. Right ventricular ejection fraction is an independent predictor of survival in patients with moderate heart failure. *J Am Coll Cardiol* 1998;32:948-954
- van Wolferen SA, Marcus JT, Boonstra A, Marques KM, Bronzwaer JG, Spreeuwenberg MD, et al. Prognostic value of right ventricular mass, volume, and function in idiopathic pulmonary arterial hypertension. *Eur Heart J* 2007;28:1250-1257
- Knauth AL, Gauvreau K, Powell AJ, Landzberg MJ, Walsh EP, Lock JE, et al. Ventricular size and function assessed by cardiac MRI predict major adverse clinical outcomes late after tetralogy of Fallot repair. *Heart* 2008;94:211-216
- Marcus FI, McKenna WJ, Sherrill D, Basso C, Bauce B, Bluemke DA, et al. Diagnosis of arrhythmogenic right ventricular cardiomyopathy/dysplasia: proposed modification of the Task Force Criteria. *Eur Heart J* 2010;31:806-814
- Oosterhof T, van Straten A, Vliegen HW, Meijboom FJ, van Dijk AP, Spijkerboer AM, et al. Preoperative thresholds for pulmonary valve replacement in patients with corrected tetralogy of Fallot using cardiovascular magnetic resonance. *Circulation* 2007;116:545-551
- Sugeng L, Mor-Avi V, Weinert L, Niel J, Ebner C, Steringer-Mascherbauer R, et al. Multimodality comparison of quantitative volumetric analysis of the right ventricle. *JACC Cardiovasc Imaging* 2010;3:10-18
- Abouzeid CM, Shah T, Johri A, Weinsaft JW, Kim J. Multimodality imaging of the right ventricle. *Curr Treat Options Cardiovasc Med* 2017;19:82
- Galea N, Carbone I, Cannata D, Cannavale G, Conti B, Galea R, et al. Right ventricular cardiovascular magnetic resonance imaging: normal anatomy and spectrum of pathological

- findings. *Insights Imaging* 2013;4:213-223
9. Prasad SK, Pennell DJ. Safety of cardiovascular magnetic resonance in patients with cardiovascular implants and devices. *Heart* 2004;90:1241-1244
 10. Dupont MV, Drăgean CA, Coche EE. Right ventricle function assessment by MDCT. *AJR Am J Roentgenol* 2011;196:77-86
 11. Koch K, Oellig F, Oberholzer K, Bender P, Kunz P, Mildenerger P, et al. Assessment of right ventricular function by 16-detector-row CT: comparison with magnetic resonance imaging. *Eur Radiol* 2005;15:312-318
 12. Lembcke A, Dohmen PM, Dewey M, Klessen C, Elgeti T, Hermann KG, et al. Multislice computed tomography for preoperative evaluation of right ventricular volumes and function: comparison with magnetic resonance imaging. *Ann Thorac Surg* 2005;79:1344-1351
 13. Raman SV, Shah M, McCarthy B, Garcia A, Ferketich AK. Multi-detector row cardiac computed tomography accurately quantifies right and left ventricular size and function compared with cardiac magnetic resonance. *Am Heart J* 2006;151:736-744
 14. Raman SV, Cook SC, McCarthy B, Ferketich AK. Usefulness of multidetector row computed tomography to quantify right ventricular size and function in adults with either tetralogy of Fallot or transposition of the great arteries. *Am J Cardiol* 2005;95:683-686
 15. Plumhans C, Mühlenbruch G, Rapae A, Sim KH, Seyfarth T, Günther RW, et al. Assessment of global right ventricular function on 64-MDCT compared with MRI. *AJR Am J Roentgenol* 2008;190:1358-1361
 16. Schroeder J, Peterschroeder A, Vaske B, Butz T, Barth P, Oldenburg O, et al. Cardiac volumetry in patients with heart failure and reduced ejection fraction: a comparative study correlating multi-slice computed tomography and magnetic resonance tomography. Reasons for intermodal disagreement. *Clin Res Cardiol* 2009;98:739-747
 17. Müller M, Teige F, Schnapauff D, Hamm B, Dewey M. Evaluation of right ventricular function with multidetector computed tomography: comparison with magnetic resonance imaging and analysis of inter- and intraobserver variability. *Eur Radiol* 2009;19:278-289
 18. Guo YK, Yang ZG, Shao H, Deng W, Ning G, Dong ZH. Right ventricular dysfunction and dilatation in patients with mitral regurgitation: analysis using ECG-gated multidetector row computed tomography. *Int J Cardiol* 2013;167:1585-1590
 19. Guo YK, Gao HL, Zhang XC, Wang QL, Yang ZG, Ma ES. Accuracy and reproducibility of assessing right ventricular function with 64-section multi-detector row CT: comparison with magnetic resonance imaging. *Int J Cardiol* 2010;139:254-262
 20. Jensen CJ, Wolf A, Eberle HC, Forsting M, Nassenstein K, Lauenstein TC, et al. Accuracy and variability of right ventricular volumes and mass assessed by dual-source computed tomography: influence of slice orientation in comparison to magnetic resonance imaging. *Eur Radiol* 2011;21:2492-2502
 21. Huang X, Pu X, Dou R, Guo X, Yan Z, Zhang Z, et al. Assessment of right ventricular function with 320-slice volume cardiac CT: comparison with cardiac magnetic resonance imaging. *Int J Cardiovasc Imaging* 2012;28 Suppl 2:87-92
 22. Takx RA, Moscariello A, Schoepf UJ, Barraza JM Jr, Nance JW Jr, Bastarrika G, et al. Quantification of left and right ventricular function and myocardial mass: comparison of low-radiation dose 2nd generation dual-source CT and cardiac MRI. *Eur J Radiol* 2012;81:e598-e604
 23. Lee H, Kim SY, Gebregziabher M, Hanna EL, Schoepf UJ. Impact of ventricular contrast medium attenuation on the accuracy of left and right ventricular function analysis at cardiac multi detector-row CT compared with cardiac MRI. *Acad Radiol* 2012;19:395-405
 24. Gao Y, Du X, Liang L, Cao L, Yang Q, Li K. Evaluation of right ventricular function by 64-row CT in patients with chronic obstructive pulmonary disease and cor pulmonale. *Eur J Radiol* 2012;81:345-353
 25. Fuchs A, Kühl JT, Lønborg J, Engstrøm T, Vejlsstrup N, Køber L, et al. Automated assessment of heart chamber volumes and function in patients with previous myocardial infarction using multidetector computed tomography. *J Cardiovasc Comput Tomogr* 2012;6:325-334
 26. Zhang XC, Yang ZG, Guo YK, Zhang RM, Wang J, Zhou DQ, et al. Assessment of right ventricular function for patients with rheumatic mitral stenosis by 64-slice multi-detector row computed tomography: comparison with magnetic resonance imaging. *Chin Med J (Engl)* 2012;125:1469-1474
 27. Yamasaki Y, Nagao M, Yamamura K, Yonezawa M, Matsuo Y, Kawanami S, et al. Quantitative assessment of right ventricular function and pulmonary regurgitation in surgically repaired tetralogy of Fallot using 256-slice CT: comparison with 3-tesla MRI. *Eur Radiol* 2014;24:3289-3299
 28. Maffei E, Messalli G, Martini C, Nieman K, Catalano O, Rossi A, et al. Left and right ventricle assessment with cardiac CT: validation study vs. cardiac MR. *Eur Radiol* 2012;22:1041-1049
 29. Wang L, Zhang Y, Yan C, He J, Xiong C, Zhao S, et al. Evaluation of right ventricular volume and ejection fraction by gated (18)F-FDG PET in patients with pulmonary hypertension: comparison with cardiac MRI and CT. *J Nucl Cardiol* 2013;20:242-252
 30. Freling HG, van Wijk K, Jaspers K, Pieper PG, Vermeulen KM, van Swieten JM, et al. Impact of right ventricular endocardial trabeculae on volumes and function assessed by CMR in patients with tetralogy of Fallot. *Int J Cardiovasc Imaging* 2013;29:625-631
 31. Goo HW, Park SH. Semiautomatic three-dimensional CT ventricular volumetry in patients with congenital heart disease: agreement between two methods with different user interaction. *Int J Cardiovasc Imaging* 2015;31:223-232
 32. Goo HW. Comparison between three-dimensional navigator-gated whole-heart MRI and two-dimensional cine MRI in

- quantifying ventricular volumes. *Korean J Radiol* 2018;19:704-714
33. Han Y, Osborn EA, Maron MS, Manning WJ, Yeon SB. Impact of papillary and trabecular muscles on quantitative analyses of cardiac function in hypertrophic cardiomyopathy. *J Magn Reson Imaging* 2009;30:1197-1202
 34. Moher D, Liberati A, Tetzlaff J, Altman DG; The PRISMA Group. Preferred reporting items for systematic reviews and meta-analyses: the PRISMA statement. *PLoS Med* 2009;6:e1000097
 35. Whiting PF, Rutjes AW, Westwood ME, Mallett S, Deeks JJ, Reitsma JB, et al. QUADAS-2: a revised tool for the quality assessment of diagnostic accuracy studies. *Ann Intern Med* 2011;155:529-536
 36. DerSimonian R, Laird N. Meta-analysis in clinical trials. *Control Clin Trials* 1986;7:177-188
 37. Williamson PR, Lancaster GA, Craig JV, Smyth RL. Meta-analysis of method comparison studies. *Stat Med* 2002;21:2013-2025
 38. Higgins JP, Thompson SG. Quantifying heterogeneity in a meta-analysis. *Stat Med* 2002;21:1539-1558
 39. Egger M, Davey Smith G, Schneider M, Minder C. Bias in meta-analysis detected by a simple, graphical test. *BMJ* 1997;315:629-634
 40. Kim KW, Lee J, Choi SH, Huh J, Park SH. Systematic review and meta-analysis of studies evaluating diagnostic test accuracy: a practical review for clinical researchers-part I. General guidance and tips. *Korean J Radiol* 2015;16:1175-1187
 41. Schwarzer G. Meta: general package for meta-analysis. Available at: <https://cran.r-project.org/package=meta>. Accessed March 15, 2019
 42. Pickett CA, Cheezum MK, Kassop D, Villines TC, Hulten EA. Accuracy of cardiac CT, radionuclide and invasive ventriculography, two- and three-dimensional echocardiography, and SPECT for left and right ventricular ejection fraction compared with cardiac MRI: a meta-analysis. *Eur Heart J Cardiovasc Imaging* 2015;16:848-852
 43. Rudski LG, Lai WW, Afilalo J, Hua L, Handschumacher MD, Chandrasekaran K, et al. Guidelines for the echocardiographic assessment of the right heart in adults: a report from the American Society of Echocardiography endorsed by the European Association of Echocardiography, a registered branch of the European Society of Cardiology, and the Canadian Society of Echocardiography. *J Am Soc Echocardiogr* 2010;23:685-713
 44. Lang RM, Badano LP, Mor-Avi V, Afilalo J, Armstrong A, Ernande L, et al. Recommendations for cardiac chamber quantification by echocardiography in adults: an update from the American Society of Echocardiography and the European Association of Cardiovascular Imaging. *Eur Heart J Cardiovasc Imaging* 2015;16:233-270
 45. Shimada YJ, Shiota M, Siegel RJ, Shiota T. Accuracy of right ventricular volumes and function determined by three-dimensional echocardiography in comparison with magnetic resonance imaging: a meta-analysis study. *J Am Soc Echocardiogr* 2010;23:943-953
 46. Dill T. Contraindications to magnetic resonance imaging: non-invasive imaging. *Heart* 2008;94:943-948
 47. Rizvi A, Deaño RC, Bachman DP, Xiong G, Min JK, Truong QA. Analysis of ventricular function by CT. *J Cardiovasc Comput Tomogr* 2015;9:1-12
 48. Gopalan D. Right heart on multidetector CT. *Br J Radiol* 2011;84:S306-S323
 49. van Hamersvelt RW, Eijsvoogel NG, Muhl C, de Jong PA, Schilham AMR, Buls N, et al. Contrast agent concentration optimization in CTA using low tube voltage and dual-energy CT in multiple vendors: a phantom study. *Int J Cardiovasc Imaging* 2018;34:1265-1275
 50. Zhang W, Ba Z, Wang Z, Lv H, Zhao J, Zhang Y, et al. Diagnostic performance of low-radiation-dose and low-contrast-dose (double low-dose) coronary CT angiography for coronary artery stenosis. *Medicine (Baltimore)* 2018;97:e11798
 51. Iyama Y, Nakaura T, Yokoyama K, Kidoh M, Harada K, Oda S, et al. Low-contrast and low-radiation dose protocol in cardiac computed tomography: usefulness of low tube voltage and knowledge-based iterative model reconstruction algorithm. *J Comput Assist Tomogr* 2016;40:941-947
 52. Scholtz JE, Ghoshhajra B. Advances in cardiac CT contrast injection and acquisition protocols. *Cardiovasc Diagn Ther* 2017;7:439-451
 53. Kerl JM, Ravenel JG, Nguyen SA, Suranyi P, Thilo C, Costello P, et al. Right heart: split-bolus injection of diluted contrast medium for visualization at coronary CT angiography. *Radiology* 2008;247:356-364
 54. Goo HW. Semiautomatic three-dimensional threshold-based cardiac computed tomography ventricular volumetry in repaired tetralogy of Fallot: comparison with cardiac magnetic resonance imaging. *Korean J Radiol* 2019;20:102-113
 55. Weinsaft JW, Cham MD, Janik M, Min JK, Henschke CI, Yankelevitz DF, et al. Left ventricular papillary muscles and trabeculae are significant determinants of cardiac MRI volumetric measurements: effects on clinical standards in patients with advanced systolic dysfunction. *Int J Cardiol* 2008;126:359-365
 56. Park EA, Lee W, Kim HK, Chung JW. Effect of papillary muscles and trabeculae on left ventricular measurement using cardiovascular magnetic resonance imaging in patients with hypertrophic cardiomyopathy. *Korean J Radiol* 2015;16:4-12